ACS APPLIED MATERIALS & INTERFACES

Research Article

www.acsami.org

Enzyme-Free Electrochemical Immunosensor Based on Host–Guest Nanonets Catalyzing Amplification for Procalcitonin Detection

Wen-Jun Shen, Ying Zhuo,* Ya-Qin Chai, Zhe-Han Yang, Jing Han, and Ruo Yuan*

Key Laboratory of Luminescent and Real-Time Analytical Chemistry, Ministry of Education, College of Chemistry and Chemical Engineering, Southwest University, Chongqing 400715, People's Republic of China

ABSTRACT: An enzyme-free electrochemical immunosensor based on the host–guest nanonets of *N,N*-bis(ferrocenoyl)-diaminoethane/*β*-cyclodextrins/poly(amidoamine) dendrimer-encapsulated Au nanoparticles (Fc-Fc/*β*-CD/PAMAM-Au) for procalcitonin (PCT) detection has been developed in this study. The signal probe was constructed as follows: amine-terminated *β*-CD was adsorbed to PAMAM-Au first, and then the prepared Fc-Fc was recognized by the *β*-CD to form stable host–guest nanonets. Next, secondary antibodies (Ab_2) were attached into the formed netlike nanostructure of Fc-Fc/*β*-CD/PAMAM–Au by chemical absorption between PAMAM-Au and -NH_2 of *β*-CD. Herein, the PAMAM-Au act not only as nanocarriers for anchoring large amounts of the *β*-CD and Ab_2 but also as nanocatalysts to catalyze the oxidation of ascorbic acid (AA) for signal amplification. Moreover, the Fc-Fc could be stably immobilized by the hydrophobic inner cavity of *β*-CD as well as improving solubility by the hydrophilic exterior of *β*-CD. With the unique structure of two ferrocene units, Fc-Fc not only affords more electroactive groups to make the electrochemical response more sensitive but also plays a role of combining dispersive *β*-CD-functionalized PAMAM-Au to form the netlike nanostructure. Furthermore, Fc-Fc exhibits good catalytic activity for AA oxidation. When the detection solution contained AA, the synergetic catalysis of PAMAM-Au and Fc-Fc to AA oxidation could be obtained, realizing enzyme-free signal amplification. The proposed immunosensor provided a linear range from 1.80 pg/mL to 500 ng/mL for PCT detection and a detection limit of 0.36 pg/mL under optimal experimental conditions. Moreover, the immunosensor has shown potential application in clinical detection of PCT.

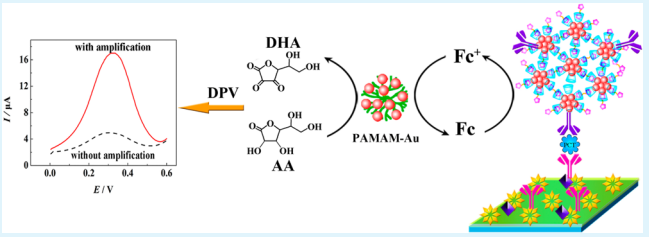

KEYWORDS: *enzyme-free electrochemical immunosensor, poly(amidoamine) dendrimer-encapsulated Au nanoparticles (PAMAM-Au), procalcitonin (PCT), β-cyclodextrin (β-CD), N,N-bis(ferrocenoyl)diaminoethane (Fc-Fc)*

1. INTRODUCTION

Procalcitonin (PCT), a 116-amino acid protein produced by C-cells of the thyroid gland, has a molecular mass of 13 kDa, which makes it a useful biomarker for early diagnosis of septicemia.[1] The PCT serum concentration is low (0.1 ng/mL) in healthy persons but increases significantly in patients with severe bacterial infections and sepsis.[2,3] Thus, PCT levels can be used for monitoring the prognosis of systemic bacterial infections and tailoring therapeutic interventions.[4] In modern society, despite varieties of analytical techniques being employed in this area,[5,6] improving the sensitivity and selectivity of PCT detection is still a challenge. Therefore, it is strongly necessary to explore novel techniques and strategies for simple, rapid, and sensitive detection of PCT.

Electrochemical immunosensors have aroused more and more interest because of their high sensitivity, simple pretreatment,[7] low cost, and fast response time.[8] Among them, enzyme-based electrochemical immunosensors have attracted special attention due to the high sensitivity based on the catalytic amplification property.[9] However, the use and selection of enzymes suffers from several disadvantages such as complex immobilization, poor stability, and high sensitivity to temperature and pH.[10] To overcome these shortages, enzyme-free electrochemical immunosensors based on nanomaterials have been developed recently. As one of the most widely used nanomaterials, Au nanoparticles (AuNPs) not only have good biocompatibility, excellent conductivity, and stability but also exhibit favorable catalytic activity.[11,12] For instance, Gu et al.[13] reported that graphene/ZnO-functionalized AuNPs exhibited distinct electrocatalytic activity to hydrogen peroxide reduction. In our previous works, we demonstrated that AuNPs as nanocatalysts could catalyze the oxidation of nicotinamide adenine dinucleotide (NADH) effectively with the help of methylene blue (MB) as redox probe.[14] Kumar et al.[15] reported that a quantum-sized AuNP-modified electrode showed excellent electrocatalytic activity toward oxidation of ascorbic acid (AA) and uric acid (UA). These previous works showed that the shape, size, and surface properties affect the catalytic activity of AuNPs. Usually, the method of preparing AuNPs is hydrothermal, which is achieved by use of $NaBH_4$ or sodium citrate to reduce

Received: November 21, 2014
Accepted: January 28, 2015
Published: January 28, 2015

DOI: 10.1021/am508137t
ACS Appl. Mater. Interfaces 2015, 7, 4127–4134

$AuCl_4^-$ solution without template. This method is simple, but it is difficult to control the particle size under 10 nm.[16] Poly(amidoamine) (PAMAM) dendrimers, which are highly branched three-dimensional macromolecules, are a promising template with precisely controllable nanosize and good structural homogeneity, which could prevent nanoparticle aggregation effectively.[17] In light of these properties, PAMAM was used as template to prepare PAMAM-encapsulated Au nanoparticles (PAMAM-Au), which showed good dispersive stability and smaller particle size compared with AuNPs prepared without template.[18] Although PAMAM-Au has been applied in electrochemical sensing such as catalyzing the oxidation of NADH[19] and reduction of H_2O_2,[20] to the best of our knowledge, this is the first time to be used as nanocatalyst to catalyze AA oxidation.

In recent years, host−guest molecular recognition has been employed in catalysis, electrochemiluminescence, and electrochemical sensing[21,22] due to its high selectivity and outstanding stability.[23] Usually, the host is a kind of molecule that contains a large-volume cavity such as β-cyclodextrins (β-CD),[24] which could load various guest molecules because of its hydrophobic internal cavity.[25,26] Ferrocene (Fc), the well-known redox probe, not only has excellent electrochemical activity and catalytic activity but also has been reported as a commonly used guest molecules for β-CD. Dubacheva et al.[27] used hyaluronic acid-functionalized β-CD to bind Fc, forming stable polymer chains based on host−guest recognition. Shang et al.[28] employed β-CD−Fc host−guest complex multifunctional Fe_3O_4 nanospheres as redox probe with the electrochemical activity of Fc. Furthermore, it was reported that Fc exhibited catalytic activity toward the oxidation of AA.[29] Inspired by these properties, we used PAMAM-Au as nanocarrires to combine amine-terminated β-CD to obtain the dispersive β-CD-functionalized PAMAM-Au (β-CD/PAMAM-Au) first, and then we designed a special Fc derivative, *N*,*N*-bis(ferrocenoyl)-diaminoethane (Fc-Fc), which could act as a bridge to bind two β-CD molecules since there are two Fc terminal groups in a molecule. With the cross-linking effect of Fc-Fc, the dispersive β-CD/PAMAM-Au was connected to nanonets for immobilizing larger amounts of Fc-Fc. Moreover, Fc-Fc not only provided more eletroactive groups for sensitive electrochemical response but also exhibited catalytic activity for oxidation of AA.

In this study, an enzyme-free electrochemical sensor based on host−guest nanonets of Fc-Fc/β-CD/PAMAM-Au catalyzing amplification for PCT detection was reported. The signal probe was constructed by these steps: First, amine-terminated β-CD was adsorbed to PAMAM-Au to obtain β-CD/PAMAM-Au. Subsequently, Fc-Fc was synthesized and introduced into the hydrophobic inner cavity of β-CD/PAMAM-Au, forming stable Fc-Fc/β-CD/PAMAM-Au host−guest nanonets as signal probe. After that, secondary antibodies (Ab_2) were attached to the formed netlike nanostructure of Fc-Fc/β-CD/PAMAM-Au. It was specially pointed out that the PAMAM-Au played dual roles: as nanocarriers, to increase the amount of immobilization of Ab_2 and β-CD, and as nanocatalysts, to catalyze the oxidation of AA efficiently. Fc-Fc exhibited three advantages: (1) it afforded a large amount of electroactive groups, making the electrochemical response more sensitive; (2) it linked PAMAM-Au/β-CD to form netlike nanostructure; and (3) it acted as catalyst to catalyze AA oxidation for signal amplification. With AA in the detection solution, enzyme-free dual signal amplification by synergetic catalysis of PAMAM-Au and Fc-Fc to AA oxidation could be realized. The fabricated immunosensor for PCT detection exhibited a low detection limit and a wide linear range. The attractive performance of the proposed electrochemical signal amplified approaches is presented in detail.

2. EXPERIMENTAL SECTION

2.1. Reagents and Materials. PCT primary monoclonal antibodies (Ab_1; 3.8 mg/mL, 1.0 mg) and secondary monoclonal antibodies (Ab_2; 2.8 mg/mL, 1.0 mg) were extracted from mice ascites. PCT (1.8 mg/mL, 1.0 mg) was recombined and expressed in *Escherichia coli*. Ab_1, Ab_2, and PCT were purchased from Kitgen Biotech Co. Ltd. (Hangzhou, China). β-Cyclodextrin (β-CD) was obtained from Binzhou Zhiyuan Bio-Tech Co. Ltd. (Shandong, China). Amine-terminated polyamidoamine (PAMAM, G5.0) dendrimer was purchased from Weihai CY Dendrimer Technology Co. Ltd. (Shandong, China), Ferrocene monocarboxylic acid (Fc-COOH), ascorbic acid (AA), gold chloride ($HAuCl_4$), and bovine serum albumin (BSA) were obtained from Sigma Chemical Co. (St. Louis, MO). *N*-(3-Dimethylaminopropyl)-*N*′-ethylcarbodiimide hydrochloride (EDC) and *N*-hydroxysuccinimide (NHS) were acquired from Shanghai Medpep Co. (Shanghai, China). Ethylenediamine and $NaBH_4$ was purchased from Ke Long Chemical Co. (Chengdu, China). Phosphate-buffered saline solution (PBS, 0.1 M) containing 10 mM Na_2HPO_4, 10 mM NaH_2PO_4, and 2 mM KCl was used as working buffer solution. Double-distilled water was used throughout this study.

2.2. Apparatus. Cyclic voltammetry (CV), differential pulse voltammetry (DPV), and electrochemical impedance spectroscopy (EIS) were carried out with a CHI 660D electrochemical workstation (Shanghai Chenhua Instrument Co.). A three-electrode system contained a platinum wire auxiliary electrode, a saturated calomel reference electrode (SCE), and glassy carbon electrode (GCE) as working electrode. The structure of nanomaterials was analyzed by Raman spectroscopy (Renishaw InVia Reflex). The sizes and morphology of various nanomaterials were investigated by S4800 scanning electron microscopy (SEM; Hitachi Co.).

2.3. Synthesis of *N*,*N*-Bis(ferrocenoyl)diaminoethane. Fc-Fc was prepared by the following method. First, 0.0575 g of Fc-COOH were dissolved in 4 mL of double-distilled water with continual ultrasonication, and then 0.5 mL of 1 mg/mL EDC and NHS (4:1) was added as coupling reagent to activate the carboxyl of Fc-COOH with the aid of stirring. Next, 10 μL of ethylenediamine was mixed with the active Fc-COOH solution under continuous stirring for 4 h. Finally, the obtained Fc-Fc was stored at 4 °C for further use.

2.4. Synthesis of Poly(amidoamine) Dendrimer-Encapsulated Au Nanoparticles. The stable PAMAM-Au was prepared with PAMAM as template according to the literature[30] with minor revision. First, 2 mL of 2 mM $HAuCl_4$ solution was added to the solution containing 20 μL of PAMAM (0.5 g/mL) with stirring for 1 h at room temperature. Subsequently, 1 mL of 20 mM $NaBH_4$ was quickly added to the above solution with vigorous stirring. When the PAMAM-Au was formed, the color of the solution changed from light yellow to light red. Finally, the obtained solution was treated with centrifugation at 12 000 rpm for 30 min, resuspended in double-distilled water, and preserved at 4 °C for further use.

2.5. Preparation of Different Labeled Ab_2 Bioconjugates. The proposed Fc-Fc/β-CD/PAMAM-Au-labeled Ab_2 bioconjugates were prepared according to the following steps. At first, 200 μL of 5 mM β-CD with NH_2 moiety was added to the prepared PAMAM-Au solutions with stirring for 4 h. Then the mixture was centrifuged for 15 min at 10 000 rpm and washed twice with distilled water. Next, 1 mL of prepared Fc-Fc was bound into the hydrophobic cavity of β-CD to form a stable host−guest inclusion complex (Fc-Fc/β-CD/PAMAM-Au) under continuous stirring. Then 100 μL of Ab_2 was added dropwise into the above mixture with stirring at 4 °C for 8 h. Finally, the proposed Ab_2/Fc-Fc/β-CD/PAMAM-Au bioconjugates were collected by centrifugation, washed several times, and then stored at 4 °C for further use.

Fc-Fc/β-CD/AuNP-labeled Ab_2 bioconjugates were prepared as follows. First, AuNPs were synthesized according to the method in

DOI: 10.1021/am508137t
ACS Appl. Mater. Interfaces 2015, 7, 4127−4134

Scheme 1. Schematic Diagram of Fabrication of Electrochemical Immunosensor[a]

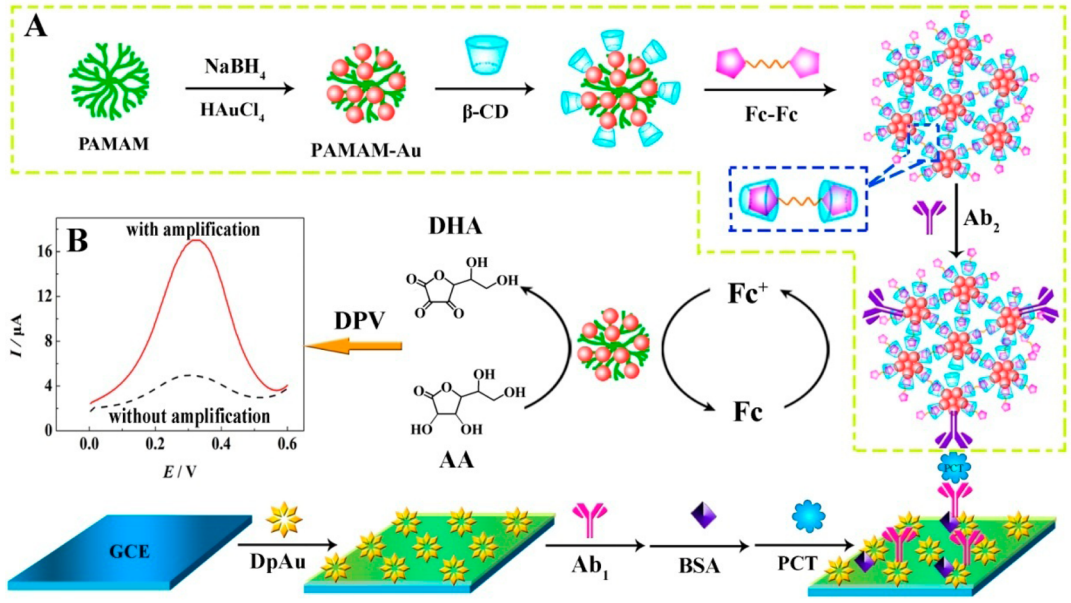

[a](A) Preparation procedure of Fc-Fc/β-CD/PAMAM-Au-labeled Ab_2 bioconjugates. (B) Comparative DPV signals with and without amplification.

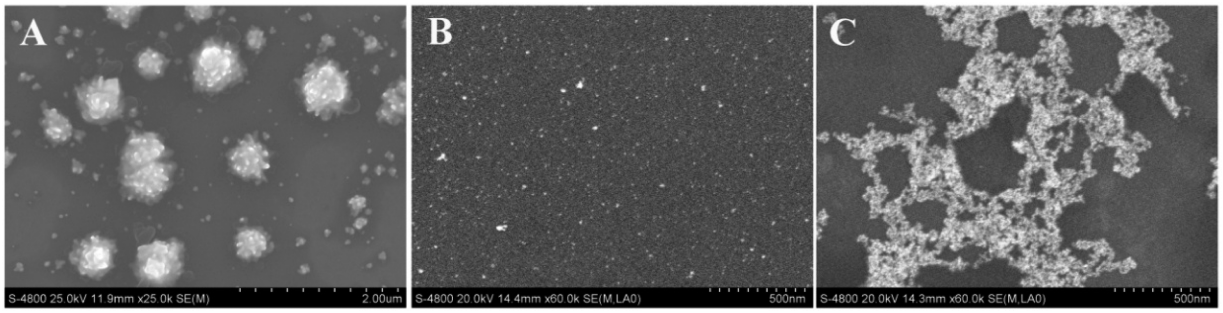

Figure 1. SEM images of (A) AuNFs, (B) PAMAM-Au and (C) Fc-Fc/β-CD/PAMAM-Au.

literature.[31] Subsequently, 200 μL of 5 mM β-CD was added to the prepared AuNPs solutions with stirring. Next, 1 mL of prepared Fc-Fc was combined into the hydrophobic cavity of β-CD under continuous stirring. Finally, 100 μL of Ab_2 was added dropwise into the mixture with stirring at 4 °C for 8 h. The Ab_2/Fc-Fc/β-CD/AuNPs were obtained after several rounds of centrifugation and stored at 4 °C for further use.

Additionally, Fc-COOH-labeled Ab_2 were synthesized with the aid of EDC and NHS as coupling agents. Briefly, 0.5 mL of 1 mg/mL EDC and NHS was added into Fc-COOH solution to activate the carboxyl. Then Ab_2 was added into the mixture, which was allowed to stay overnight at 4 °C with continuous stirring. Next, it was centrifuged for 15 min at 12 000 rpm, washed twice with PBS, and then stored at 4 °C for further use.

2.6. Fabrication of Immunosensor. First, the GCE (Φ = 4 mm) was polished with 0.3 and 0.05 μm alumina and ultrasonicated in double-distilled water to obtain a mirrorlike surface. To attach Ab_1, an Au nanoflower (AuNF) modified layer was obtained by electrochemical deposition in 2 mL of 1% $HAuCl_4$ under a potential of −0.2 V for 30 s. The AuNF/GCE electrode was incubated for 12 h at 4 °C with 20 μL of Ab_1. After the modified electrode was washed with PBS (pH 7.4), BSA as a blocking reagent was incubated for 40 min to eliminate nonspecific binding effects. Finally, the immunosensor was rinsed with distilled water and stored at 4 °C when not in use.

2.7. Detection Principle of Immunosensor. A sandwich reaction was used to detect PCT with DPV. The DPV parameters applied were 50 mV·s^{-1} sweeping rate, 50 ms pulse width, 0.2 s pulse period, and voltage range from 0 to 0.8 V. On the basis of a sandwich format, the as-prepared immunosensor was first incubated with 20 μL of PCT standard solution at 35 °C for 50 min and then incubated with 20 μL of Ab_2 bioconjugates for about 1 h. The electrode fabrication of immunosensor is shown in Scheme 1.

3. RESULTS AND DISCUSSION

3.1. Characterization of Different Nanomaterials by Scanning Electron Microscopy. Figure 1A shows the SEM image of Au nanoflowers (AuNFs): it can be seen that $HAuCl_4$ electrodeposition on bare GCE presented a nanoflowerlike shape. Figure 1B shows the SEM image of PAMAM-Au. It was shown that the PAMAM-Au displayed good dispersive stability, and the particle size of PAMAM-Au was about 5−10 nm, which illustrated that the preparation of PAMAM-Au by using PAMAM as template had better controllable nanoparticle size. Figure 1C shows the SEM image of Fc-Fc/β-CD/PAMAM-Au,;it can be seen that β-CD/PAMAM-Au formed extended nanonets with the introduction of Fc-Fc, indicating the stable host−guest nanonets of Fc-Fc/β-CD/PAMAM-Au were synthesized successfully.

3.2. Raman Spectra of Different Nanomaterials. Raman spectroscopy is usually applied to structure analysis, key state characteristic analysis, and qualitative identification.[32] Here,

DOI: 10.1021/am508137t
ACS Appl. Mater. Interfaces 2015, 7, 4127−4134

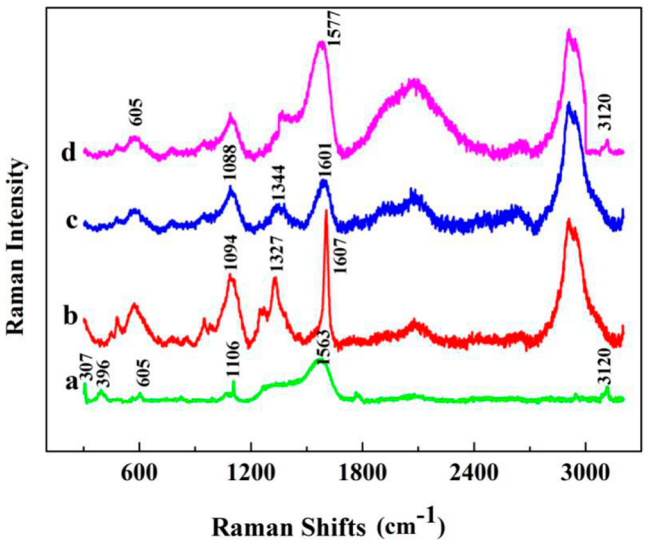

Figure 2. Raman spectra of (a) Fc-Fc, (b) β-CD, (c) β-CD/PAMAM-Au, and (d) Fc-Fc/β-CD/PAMAM-Au.

Figure 2 displays the Raman spectra of Fc-Fc (curve a), β-CD (curve b), β-CD/PAMAM-Au (curve c), and Fc-Fc/β-CD/PAMAM-Au (curve d). For curve a, three characteristic peaks of Fc can be seen at 307, 396, and 1106 cm^{-1}.[33] Particularly, the peaks at 307 and 396 cm^{-1} belong to the Fc ring stretch and ring tilt,[34] respectively. Furthermore, three evident peaks were obtained at 605, 1653, and 3120 cm^{-1}, which were assigned to amide VI, I, and B,[35] respectively. These Raman data illustrated that Fc-Fc was successfully synthesized through an amide bond. Curve b shows the characteristic peaks of β-CD; the strong intensity peaks at 1094, 1327, and 1607 cm^{-1} were attributable to C−C stretching, C−H deformation vibration, and aromatic C≡C stretching, respectively, which was in agreement with that reported in previous works.[36] After PAMAM-Au was combined with β-CD (curve c), the peaks at 1094, 1327, and 1607 cm^{-1} shifted to 1088, 1344, and 1601 cm^{-1}, respectively, which suggested that the amine-terminated β-CD bound to the PAMAM-Au surface via N−Au bonds. Moreover, the intensity of these peaks was reduced slightly,because the unique dendritic structures of PAMAM lengthened the distance between PAMAM-Au and β-CD. Curve d is the Raman spectrum of Fc-Fc/β-CD/PAMAM-Au; it can be seen that the characteristic peaks of Fc (307, 396, and 1106 cm^{-1}) disappeared while the characteristic peaks of amide VI (605 cm^{-1}), I (1653 cm^{-1}), and B (3120 cm^{-1}) are still present. Obviously, the peak at 1577 cm^{-1} of Fc-Fc/β-CD/PAMAM-Au seemed to result from overlap of the Fc-Fc peak at 1563 cm^{-1} and the β-CD peak at 1607 cm^{-1}. From the results, it can be inferred that Fc was introduced into the hydrophobic inner cavity of β-CD/PAMAM-Au, while the amide bond was outside of the hydrophobic inner cavity of β-CD/PAMAM-Au.

3.3. Electrochemical Characterization of Immunosensor. CV and EIS were convenient and valuable techniques to monitor the stepwise fabrication of the immunosensor. Figure 3A shows the CVs of electrode modification in the presence of 5 mM $[Fe(CN)_6]^{3-/4-}$ as redox probe in 0.1 M PBS (pH 7.4) containing 0.1 M KCl from −0.2 to 0.6 V at a scan rate of 100 $mV{\cdot}s^{-1}$. It can be seen that bare GCE showed a pair of typical reversible redox peaks (curve a). With electrodeposition of AuNFs, the resulting electrode exhibited increasing current (curve b) since AuNFs could accelerate the electron transfer and give a larger electrochemical surface area. Subsequently, with the assembly of Ab_1 (curve c), the redox peak current decreased due to the hindering effect of protein on electron transfer. After the employment of BSA to block nonspecific sites, a further decrease of redox peak current was obtained (curve d). Finally, the peak currents apparently decreased (curve e) upon incubation with PCT solution; the reason was that formation of Ab_1−PCT complex hindered electron transfer. In order to illustrate the electrochemical behavior after the immunosensor was incubated with Fc-Fc/β-CD/PAMAM-Au-labeled Ab_2, CV curves of PCT/BSA/Ab_1/AuNFs/GCE were scanned in PBS, pH 7.4, before and after incubation with Fc-Fc/β-CD/PAMAM-Au-labeled Ab_2. As shown in the top left side of Figure 2A, the electrode of PCT/BSA/Ab_1/AuNF/GCE (curve e) showed no redox peak in PBS. When Fc-Fc/β-CD/PAMAM-Au-labeled Ab_2 was incubated with the electrode (curve f), a pair of redox peaks (assigned to the signal of Fc-Fc) was exhibited in the range of 0.2−0.4 V, which showed that Fc-Fc/β-CD/PAMAM-Au-labeled Ab_2 was reacted with PCT successfully.

Electrochemical impedance spectroscopy can also be used to study the interface properties of the surface-modified electrodes. Figure 3B illustrates EIS of the fabricated immunosensor during stepwise modification in the presence of 5.0 mM $[Fe(CN)_6]^{3-/4-}$ within the frequency range 10^{-2}−10^6 Hz at a formal potential of 220 mV. The bare GCE displayed a small semicircle (curve a). After AuNFs were electrodeposited on the

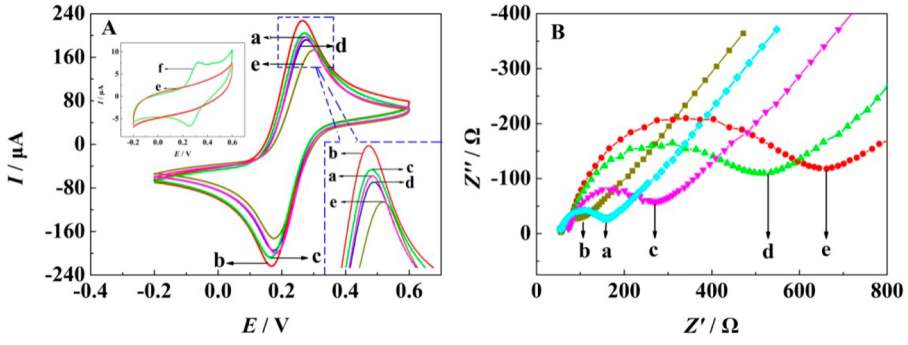

Figure 3. (A) Cyclic voltammetry and (B) electrochemical impedance spectroscopy of different modified electrodes in PBS, pH 7.4, containing 5.0 mM $[Fe(CN)_6]^{3-/4-}$ as redox probe: (a) bare GCE, (b) AuNF/GCE, (c) Ab_1/AuNF/GCE, (d) BSA/Ab_1/AuNF/GCE, (e) PCT/BSA/Ab_1/AuNF/GCE. (A, inset) CV of different modified electrodes in PBS, pH 7.4: (e) PCT/BSA/Ab_1/AuNF/GCE and (f) Fc-Fc/β-CD/PAMAM-Au-labeled Ab_2/PCT/BSA/Ab_1/AuNF/GCE.

DOI: 10.1021/am508137t
ACS Appl. Mater. Interfaces 2015, 7, 4127−4134

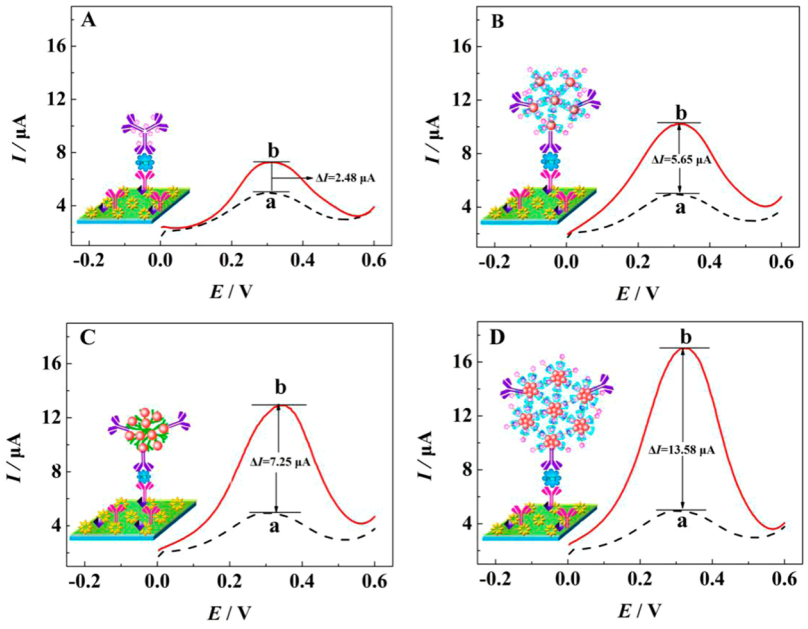

Figure 4. Differential pulse voltammetry of immunosensors with different labeled Ab_2 bioconjugates, (A) Fc-COOH-labeled Ab_2, (B) Fc-Fc/β-CD/AuNP-labeled Ab_2, (C) PAMAM-Au-labeled Ab_2, and (D) Fc-Fc/β-CD/PAMAM-Au-labeled Ab_2, based on assay toward blank (curve a) and 1.8 ng/mL PCT (curve b) in a standard sandwich format.

electrode, R_{et} decreased significantly (curve b), owing to the conductive property of AuNFs, and then increased R_{et} was acquired (curve c), which implied that Ab_1 was immobilized onto the AuNF films and could hinder the transmission of electrons across the electrode surface. Moreover, the R_{et} kept increasing after incubation with BSA and PCT (curves d and e, respectively), which was attributed to the fact that BSA and PCT insulated the conductive support and bound the interfacial electron transfer.

3.4. Amplification Properties of Various Labeled Ab_2 Bioconjugates. To investigate the amplification properties of various labeled Ab_2 bioconjugates, the contrast experiment to compare the DPV responses before and after signal amplification under the same conditions was conducted. Four kinds of various labeled Ab_2 bioconjugates were prepared: Fc-COOH-labeled Ab_2 (Figure 4A), Fc-Fc/β-CD/AuNP-labeled Ab_2 (Figure 4B), PAMAM-Au-labeled Ab_2 (Figure 4C), and Fc-Fc/β-CD/PAMAM-Au-labeled Ab_2 (Figure 4D). The same batch of immunosensors was incubated with 1.80 ng/mL PCT and then incubated with different labeled Ab_2 bioconjugates. As shown in Figure 4A, the DPV response of the immunosensor with Fc-COOH-labeled Ab_2 was raised about 2.48 μA compared with background signal (DPV response of BSA/Ab_1/AuNF/GCE); this was because Fc-COOH possessed excellent redox properties and exhibited good catalytic activity toward the oxidation of AA. Then about 5.65 μA increased DPV response was shown by the immunosensor with Fc-Fc/β-CD/AuNP-labeled Ab_2 (Figure 4B). The reason was that a large amount of Fc-Fc was obtained, which afforded more electroactive groups to catalyze the AA oxidation for signal amplification. In Figure 4C, the DPV response of the immunosensor with PAMAM-Au-labeled Ab_2 was raised about 7.25 μA, which showed that PAMAM-Au was a good nanocatalyst to catalyze the oxidation of AA efficiently. When the immunosensor was incubated with Fc-Fc/β-CD/PAMAM-Au-labeled Ab_2, the DPV response was raised about 13.58 μA (Figure 4D). The enhancement could be attributed to the synergetic catalysis of PAMAM-Au and Fc-Fc to the AA oxidation, resulting in further amplification of the signal.

3.5. Optimization of Immunosensor Experimental Conditions. The goal of this study was to control the optimal experimental conditions to obtain the best performance of the proposed immunosensors for 1.80 ng/mL PCT detection. Several key parameters, such as concentration of AA in detection solution, pH of detection solution, incubation time, and temperature of PCT were investigated by altering each variable in turn while keeping the others constant. These optimization experiments were performed by monitoring the currents with DPV measurement.

The concentration of AA in detection solution was a key parameter influencing the response of the immunosensor, which was evaluated by the immunosensor incubated with 1.80 ng/mL PCT in pH 7.5 detection solution. Figure 5A shows that the oxidation peak current increased obviously with increasing concentration of AA and then tended to a constant while the AA concentration was 1.40 mM. Therefore, 1.40 mM AA was chosen as the optimized concentration.

As the pH of the detection solution might affect not only electrochemical performance of Fc-Fc and AA but also activity of the immobilized immunoproteins, pH dependence of the voltammetric response was examined over pH values from 4.5 to 9.5 in detection solution containing 1.4 mM AA (Figure 5B). The results indicated that the strongest peak current response was obtained at pH 7.5. Thus, detection solution of pH 7.5 was selected in the following experiments.

The effect of incubation time (Figure 5C) was also studied. The immunosensor was incubated with 20 μL of 1.80 ng/mL PCT for different times from 10 to 60 min. It was found that current increased with incubation time up to 50 min, and after that the increase slowed down significantly. Consequently, 50 min was chosen as the optimal incubation time of PCT.

Incubation temperature of PCT had an important effect on the immunosensor. Figure 5D shows the peak current response was improved with the temperature increasing to 35 °C and then

DOI: 10.1021/am508137t
ACS Appl. Mater. Interfaces 2015, 7, 4127−4134

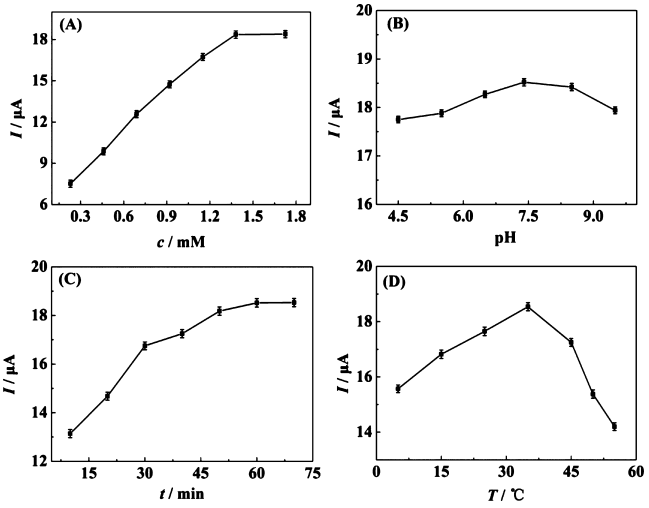

Figure 5. Optimization of experimental parameters: (A) Influence of AA concentrations on the immunosensor after incubation with 1.80 ng/mL PCT. (B) Effect of pH of detection solution containing 1.4 mM AA. (C) Effect of different incubation times after the immunosensor was incubated with 1.80 ng/mL PCT solution in pH 7.4 detection solution containing 1.4 mM AA. (D) Influence of incubation temperature when immune-reacted with 1.80 ng/mL PCT.

reduced with the temperature over 35 °C, which meant 35 °C would be taken to form the most immunocomplexes between PCT and anti-PCT on the electrode surface. Therefore, 35 °C was adopted as the optimal incubation temperature

3.6. Performance of Immunosensor. *3.6.1. Differential Pulse Voltammetry Response and Calibration Curves.* Under the optimal experimental conditions, the prepared immunosensors were employed to detect PCT with various concentrations. As seen in Figure 6, the DPV signal increased

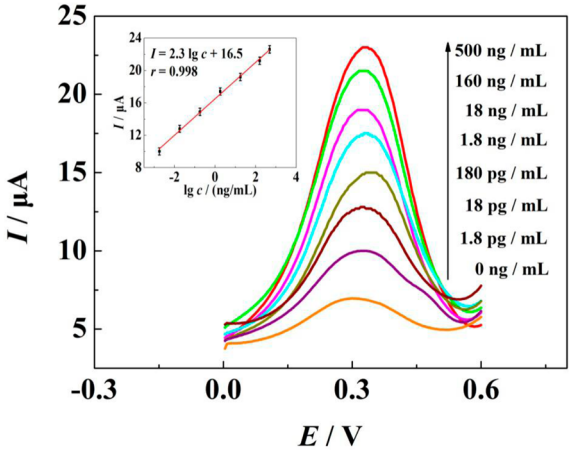

Figure 6. DPV responses and calibration curve (inset) of prepared immunosensor with PCT at different concentrations.

with increasing PCT concentration and showed a good linear relationship with the logarithm of PCT from 1.80 pg/mL to 500 ng/mL. The regression equation was $I = 2.3 \log c + 16.5$ (where I is current and c is concentration of PCT) with a correlation coefficient of 0.998 and a detection limit of 0.36 pg/mL (signal/noise = 3). According to the linear equation, quantitative detection of PCT could be achieved. Moreover, the detection limit and linear range of other PCT immunosensors are shown in Table 1.[37−39] Compared with these previous reports, the immunosensor exhibited lower detection limit and wider linear range.

Table 1. Comparison of Other PCT Detection Methods Based on Sandwich Formation

detection method[a]	detection limit, (pg·mL^{-1})	linear range, (ng·mL^{-1})	ref
EC	5.00×10^{-1}	(1.00×10^{-2})−350	37
ECL	3.40	(1.00×10^{-2})−20.0	38
EC	4.30×10^{-1}	(1.00×10^{-3})−20.0	39
EC	3.60×10^{-1}	(1.80×10^{-3})−500	our work

[a]EC, electrochemical; ECL, electrochemiluminescence.

3.6.2. Stability, Selectivity, and Reproducibility of Immunosensor. Long-term storage stability of the proposed immunosensor was investigated over a period of 30 days of storage (at 4 °C). It was observed that 91.4% of the initial current remained after 15 days and 83.7% after 30 days, which showed satisfying stability of the immunosensor.

Possible interfering substances were used to elevate the selectivity of immunosensor for PCT detection (Figure 7).

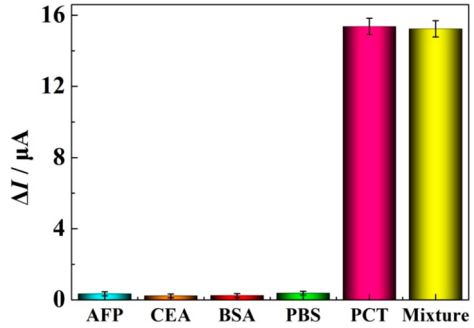

Figure 7. Selectivity of immunosensor investigated by incubation in the following samples under the same conditions: 10 ng/mL AFP; 10 ng/mL CEA; 10 ng/mL BSA; 10 ng/mL PBS; 10 ng/mL PCT; and a mixture of these.

The selectivity experiments were performed by using alpha-1-fetoprotein, (AFP, 10 ng/mL), carcinoembryonic antigen (CEA, 10 ng/mL), BSA (10 ng/mL), and PBS (10 ng/mL) to replace the PCT (10 ng/mL), respectively. It was found that almost no signal change was obtained compared with the background. Additionally, the immunosensor was also incubated with 10 ng/mL PCT containing a mixture of different interfering species, no significant difference was found compared with the current obtained from 10 ng/mL PCT only, indicating a good selectivity of the proposed immunosensor.

The reproducibility of the immunosensor was investigated by analysis of the same concentration of PCT (1.8 ng/mL) with four prepared electrodes under the same conditions. The four electrodes presented closely similarDPV responses with an acceptable relative standard deviation (RSD) of 3.7% (n = 4).

3.6.3. Real Sample Analysis of Procalcitonin. The feasibility of the electrochemical immunosensor for clinical applications was examined by the standard addition method (adding PCT of different standard concentrations to normal human serum samples diluted 50 times with 0.1 M PBS, pH 7.4). As shown in Table 2, the recovery was acceptable, ranging from 92.3% to 103.3%. The result suggested that the proposed immunosensor was available for detection of PCT in real samples.

DOI: 10.1021/am508137t
ACS Appl. Mater. Interfaces 2015, 7, 4127−4134

Table 2. Recovery of Proposed Immunosensor in Normal Human Serum

serum sample	added PCT ($ng \cdot mL^{-1}$)	found PCT ($ng \cdot mL^{-1}$)	recovery (%)
1	3.60×10^{-3}	3.72×10^{-3}	103.3
2	3.60×10^{-2}	3.47×10^{-2}	96.40
3	3.60×10^{-1}	3.51×10^{-1}	97.50
4	3.60	3.66	101.6
5	36.0	33.2	92.30

4. CONCLUSIONS

In conclusion, we have developed an enzyme-free electrochemical immunosensor for efficient detection of PCT based on host−guest nanonets of Fc-Fc/β-CD/PAMAM-Au catalyzing amplification. PAMAM-Au was used for loading a large amount of Ab_2 and β-CD as nanocarriers and catalyzing the oxidation of AA as nanocatalyst. Fc-Fc not only increased the amount of electroactive groups and made the electrochemical response more sensitive but also linked dispersed β-CD/PAMAM-Au to form a netlike structure. Moreover, enzyme-free signal enhancement could be obtained by the synergetic catalysis of Fc-Fc and PAMAM-Au toward AA oxidation. The proposed immunosensor exhibited wide linear range, low detection limit, favorable reproducibility, and satisfactory sensitivity. Therefore, this enzyme-free signal-amplified electrochemical immunosensor provides a new opportunity for sensitive detection of PCT.

AUTHOR INFORMATION

Corresponding Authors

*Telephone +86-23-68252277; fax +86-23-68253172; e-mail yingzhuo@swu.edu.cn.

*Telephone +86-23-68252277; fax +86-23-68253172; e-mail yuanruo@swu.edu.cn.

Notes

The authors declare no competing financial interest.

ACKNOWLEDGMENTS

This research was supported by NNSF of China (21275119, 21105081, 51473136), Research Fund for the Doctoral Program of Higher Education (RFDP) (20110182120010), Ministry of Education of China (Project 708073), Specialized Research Fund for the Doctoral Program of Higher Education (20100182110015), Natural Science Foundation Project of Chongqing City (CSTC-2011BA7003, CSTC-2014JCYJA20005), and Fundamental Research Funds for the Central Universities (XDJK2013A027, XDJK2014A012), China.

REFERENCES

(1) Assicot, M.; Gendrel, D.; Carsin, H.; Raymond, J.; Guilbaud, J.; Bohuon, C. High Serum Procalcitonin Concentrations in Patients with Sepsis and Infection. *Lancet* **1993**, *341*, 515−518.

(2) Russwurm, S.; Wiederhold, M.; Oberhoffer, M.; Stonans, I.; Zipfel, P. F.; Reinhart, K. Molecular Aspects and Natural Source of Procalcitonin. *Clin. Chem. Lab. Med.* **1999**, *37*, 789−797.

(3) Karzai, W.; Oberhoffer, M.; Meier-Hellmann, A.; Reinhart, K. Procalcitonin − A New Indicator of the Systemic Response to Severe Infections. *Infection* **1997**, *25*, 329−334.

(4) Wacker, C.; Prkno, A.; Brunkhorst, F. M.; Schlattmann, P. Procalcitonin as a Diagnostic Marker for Sepsis: A Systematic Review and Meta-analysis. *Lancet Infect. Dis.* **2013**, *13*, 426−435.

(5) Heyland, D. K.; Johnson, A. P.; Reynolds, S. C. Procalcitonin for Reduced Antibiotic Exposure in the Critical Care Setting: A Systematic Review and an Economic Evaluation. *Crit. Care. Med.* **2011**, *39*, 1792−1799.

(6) Muroi, C.; Lemb, J. B.; Hugelshofer, M.; Seule, M.; Bellut, D.; Keller, E. Early Systemic Procalcitonin Levels in Patients with Aneurysmal Subarachnoid Hemorrhage. *Neurocrit. Care.* **2014**, *21*, 73−77.

(7) Chikkaveeraiah, B. V.; Bhirde, A. A.; Morgan, N. Y.; Eden, H. S.; Chen, X. Y. Electrochemical Immunosensors for Detection of Cancer Protein Biomarkers. *ACS Nano* **2012**, *6*, 6546−6561.

(8) Chen, S.; Sun, G. High Sensitivity Ammonia Sensor Using a Hierarchical Polyaniline/poly(ethylene-*co*-glycidyl methacrylate) Nanofibrous Composite Membrane. *ACS Appl. Mater. Interfaces* **2013**, *5*, 6473−6477.

(9) Fang, B.; Gu, A. X.; Wang, G. F.; Wang, W.; Feng, Y. H.; Zhang, C. H.; Zhang, X. J. Silver Oxide Nanowalls Grown on Cu Substrate as an Enzymeless Glucose Sensor. *ACS Appl. Mater. Interfaces* **2009**, *1*, 2829−2834.

(10) Strack, G.; Bocharova, V.; Arugula, M. A.; Pita, M.; Halámek, J.; Katz, J. Towards Biochemical Filters with a Sigmoidal Response to pH Changes: Buffered Biocatalytic Signal Transduction. *Phys. Chem. Lett.* **2010**, *1*, 839−843.

(11) Devan, R. S.; Patil, R. A.; Lin, J. H.; Ma, Y. R. One-Dimensional Metal−Oxide Nanostructures: Recent Developments in Synthesis, Characterization and Applications. *Adv. Funct. Mater.* **2012**, *22*, 3326−3370.

(12) Walsh, M. J.; Yoshida, K.; Kuwabara, A.; Pay, M. L.; Gai, P. L.; Boyes, E. D. On the Structural Origin of the Catalytic Properties of Inherently Strained Ultrasmall Decahedral Gold Nanoparticles. *Nano Lett.* **2012**, *12*, 2027−2031.

(13) Gu, H.; Yang, Y.; Tian, J. X.; Shi, G. Y. Photochemical Synthesis of Noble Metal (Ag, Pd, Au, Pt) on Graphene/ZnO Multihybrid Nanoarchitectures as Electrocatalysis for H_2O_2Reduction. *ACS Appl. Mater. Interfaces* **2013**, *5*, 6762−6768.

(14) Yi, H. Y.; Xu, W. J.; Yuan, Y. L.; Wu, Y. M.; Chai, Y. Q.; Yuan, R. A Sensitive Electrochemical Aptasensor for Thrombin Detection Based on Exonuclease-catalyzed Target Recycling and Enzyme-catalysis. *Biosens. Bioelectron.* **2013**, *47*, 368−372.

(15) Kumar, S. S.; Kwak, K.; Lee, D. Electrochemical Sensing Using Quantum-sized Gold Nanoparticles. *Anal. Chem.* **2011**, *83*, 3244−3247.

(16) Brust, M.; Gordillo, G. J. Electrocatalytic Hydrogen Redox Chemistry on Gold Nanoparticles. *J. Am. Chem. Soc.* **2012**, *134*, 3318−3321.

(17) Wang, L.; Erasquin, U. J.; Zhao, M. R.; Ren, L.; Zhang, M. Y.; Cheng, G. J.; Wang, Y. J.; Cai, C. Z. Stability, Antimicrobial Activity, and Cytotoxicity of Poly(amidoamine) Dendrimers on Titanium Substrates. *ACS Appl. Mater. Interfaces* **2011**, *3*, 2885−2894.

(18) Zong, J.; Yang, X. L.; Trinchi, A.; Hardin, S.; Cole, I.; Zhu, Y. H.; Li, C. Z.; Muster, T.; Wei, G. Photoluminescence Enhancement of Carbon Dots by Gold Nanoparticles Conjugated via PAMAM Dendrimers. *Nanoscale* **2013**, *5*, 11200−11206.

(19) Zhang, Q.; Wang, N.; Zhao, L. B.; Xu, T. W.; Cheng, Y. Y. Polyamidoamine Dendronized Hollow Fiber Membranes in the Recovery of Heavy Metal Ions. *ACS Appl. Mater. Interfaces* **2013**, *5*, 1907−1912.

(20) Zhu, J. Y.; Zheng, L. F.; Wen, S. H.; Tang, Y. Q.; Shen, M. W.; Zhang, G. X.; Shi, X. Y. Targeted Cancer Theranostics Using Alpha-tocopheryl Succinate-conjugated Multifunctional Dendrimer-entrapped Gold Nanoparticles. *Biomaterials* **2014**, *35*, 7635−7646.

(21) Yang, H.; Yuan, B.; Zhang, X. Supramolecular Chemistry at Interfaces: Host−Guest Interactions for Fabricating Multifunctional Biointerfaces. *Acc. Chem. Res.* **2014**, *47*, 2106−2115.

(22) Han, J.; Zheng, Y. C.; Zheng, S.; Li, S. P.; Hu, T. N.; Tang, A. J.; Gao, C. Water Soluble Octa-functionalized POSS: All-click Chemistry Synthesis and Efficient Host−guest Encapsulation. *Chem. Commun.* **2014**, *50*, 8712−8714.

(23) Peng, T.; Paramelle, D.; Sana, B.; Lee, C. F.; Lim, S. Designing Non-Native Iron-Binding Site on a Protein Cage for Biological Synthesis of Nanoparticles. *Small* **2014**, *10*, 3131−3138.

DOI: 10.1021/am508137t
ACS Appl. Mater. Interfaces 2015, 7, 4127−4134

(24) Wang, L. S.; Lei, J. P.; Ma, R. N. Host-guest Interaction of Adamantine with a β-cyclodextrin-functionalized AuPd Bimetallic Nanoprobe for Ultrasensitive Electrochemical Immunoassay of Small Molecules. *Anal. Chem.* **2013**, *13*, 6505−6510.
(25) Kakuta, T.; Takashima, Y.; Nakahata, M.; Otsubo, M.; Yamaguchi, H.; Harada, A. Preorganized Hydrogel: Self-Healing Properties of Supramolecular Hydrogels Formed by Polymerization of Host−Guest-Monomers that Contain Cyclodextrins and Hydrophobic Guest Groups. *Adv. Mater.* **2013**, *25*, 2849−2853.
(26) Tamesue, S.; Takashima, Y.; Yamaguchi, H.; Shinkai, S.; Harada, A. Photoswitchable Supramolecular Hydrogels Formed by Cyclodextrins and Azobenzene Polymers. *Angew. Chem., Int. Ed.* **2010**, *122*, 7623−7626.
(27) Dubacheva, G. V.; Curk, T.; Mognetti, B. M.; Auzely-Veltý, R.; Frenkel, D.; Richter, R. P. Superselective Targeting Using Multivalent Polymers. *J. Am. Chem. Soc.* **2014**, *136*, 1722−1725.
(28) Shang, K.; Wang, X. D.; Sun, B.; Cheng, Z. Q.; Ai, S. Y. β-cyclodextrin-ferrocene Host−guest Complex Multifunctional Labeling Triple Amplification Strategy for Electrochemical Immunoassay of Subgroup J of Avian Leukosis Viruses. *Biosens. Bioelectron.* **2013**, *45*, 40−45.
(29) Wang, J. Y.; Chen, L. C.; Ho, K. C. Synthesis of Redox Polymer Nanobeads and Nanocomposites for Glucose Biosensors. *ACS Appl. Mater. Interfaces* **2013**, *5*, 7852−7861.
(30) Zhang, Q.; Wang, N.; Zhao, L. B.; Xu, T. W.; Cheng, Y. Y. Polyamidoamine Dendronized Hollow Fiber Membranes in the Recovery of Heavy Metal Ions. *ACS Appl. Mater. Interfaces* **2013**, *5*, 1907−1912.
(31) Sau, T. K.; Rogach, A. L.; Jäckel, F.; Klar, T. A.; Feldmann, J. Properties and Applications of Colloidal Nonspherical Noble Metal Nanoparticles. *Adv. Mater.* **2010**, *22*, 1805−1825.
(32) Arjunana, V.; Anithab, R.; Devic, L.; Mohand, S.; Yang, H. F. Comprehensive Quantum Chemical and Spectroscopic (FTIR, FT-Raman, ^{1}H, ^{13}C NMR) Investigations of (1,2-Epoxyethyl)benzene and (1,2-Epoxy-2-phenyl)propane. *Spectrochim. Acta, Part A* **2015**, *135*, 120−136.
(33) Heise, H. M.; Kuckuk, R.; Bereck, A.; Riegel, D. Infrared Spectroscopy and Raman Spectroscopy of Cyclodextrin Derivatives and Their Ferrocene Inclusion Complexes. *Vib. Spectrosc.* **2010**, *53*, 19−23.
(34) Chen, Y.; Klimczak, A.; Galoppini, E.; Lockard, J. V. Structural Interrogation of a Cucurbit[7]uril-ferrocene Host−guest Complex in the Solid State: A Raman Spectroscopy Study. *RSC Adv.* **2013**, *3*, 1354−1358.
(35) Shi, Y. B.; Fang, J. L.; Liu, X. Y.; Du, L.; Tang, W. X. Fourier Transform IR and Fourier Transform Raman Spectroscopy Studies of Metallothionein-III: Amide I Band Assignments and Secondary Structural Comparison with Metallothioneins-I and -II. *Biopolymers* **2002**, *65*, 81−88.
(36) Krishna Mohan, P. R.; Sreelakshmi, G.; Muraleedharan, C. V.; Joseph, R. Water Soluble Complexes of Curcumin with Cyclodextrins: Characterization by FT-Raman Spectroscopy. *Vib. Spectrosc.* **2012**, *62*, 77−84.
(37) Fang, Y. S.; Wang, H. Y.; Wang, L. S.; Wang, J. F. An Enhanced Sensitive Electrochemical Immunosensor Based on Efficient Encapsulation of Enzyme in Silica Matrix for the Detection of Human Immunodeficiency Virus p24. *Biosens. Bioelectron.* **2015**, *64*, 324−332.
(38) Li, H. N.; Sun, Y. Y.; Elseviers, J.; Muyldermans, S.; Liu, S. Q.; Wan, Y. K. A Nanobody-based Electrochemiluminescent Immunosensor for Sensitive Detection of Human Procalcitonin. *Analyst* **2014**, *139*, 3718−3721.
(39) Liu, F.; Xiang, G. M.; Yuan, R.; Chen, X. M.; Luo, F. K.; Jiang, D. N.; Huang, S. G.; Li, Y.; Pu, X. Y. Procalcitonin Sensitive Detection Based on Graphene−Gold Nanocomposite Film Sensor Platform and Single-walled Carbon Nanohorns/Hollow Pt Chains Complex as Signal Tags. *Biosens. Bioelectron.* **2014**, *60*, 210−217.

DOI: 10.1021/am508137t
ACS Appl. Mater. Interfaces 2015, 7, 4127−4134